Double-Electromagnetically-Induced-Transparency Ground-State Cooling of Stationary Two-Dimensional Ion Crystals

Mu Qiao,[1,*] Ye Wang,[1,2] Zhengyang Cai,[1] Botao Du,[1,4] Pengfei Wang,[1] Chunyang Luan,[1] Wentao Chen,[1] Heung-Ryoul Noh,[3] and Kihwan Kim[1,†]

[1]*Center for Quantum Information, Institute for Interdisciplinary Information Sciences, Tsinghua University, Beijing 100084, People's Republic of China*

[2]*Department of Electrical and Computer Engineering, Duke University, Durham, North Carolina 27708, USA*

[3]*Department of Physics, Chonnam National University, Gwangju 61186, Korea*

[4]*Department of Physics and Astronomy, Purdue University, West Lafayette, Indiana 47907, USA*

(Received 27 March 2020; accepted 21 December 2020; published 13 January 2021)

We theoretically and experimentally investigate double-electromagnetically-induced transparency (double-EIT) cooling of two-dimensional ion crystals confined in a Paul trap. The double-EIT ground-state cooling is observed for $^{171}Yb^{+}$ ions with a clock state, for which EIT cooling has not been realized like many other ions with a simple Λ scheme. A cooling rate of $\dot{\bar{n}} = 34(\pm 1.8)$ ms^{-1} and a cooling limit of $\bar{n} = 0.06(\pm 0.059)$ are observed for a single ion. The measured cooling rate and limit are consistent with theoretical predictions. We apply double-EIT cooling to the transverse modes of two-dimensional (2D) crystals with up to 12 ions. In our 2D crystals, the micromotion and the transverse mode directions are perpendicular, which makes them decoupled. Therefore, the cooling on transverse modes is not disturbed by micromotion, which is confirmed in our experiment. For the center of mass mode of a 12-ion crystal, we observe a cooling rate and a cooling limit that are consistent with those of a single ion, including heating rates proportional to the number of ions. This method can be extended to other hyperfine qubits, and near ground-state cooling of stationary 2D crystals with large numbers of ions may advance the field of quantum information sciences.

DOI: 10.1103/PhysRevLett.126.023604

Cooling down mechanical oscillators into their ground states facilitates experimental investigations and applications with atoms and ions for quantum information sciences [1]. Quantized vibrations of mechanical oscillators can be used as resources for continuous-variable quantum computation [2–6] or boson sampling [7–12], which begins with ground-state preparation. In order to demonstrate quantum advantages with these applications, ground-state cooling dozens of vibrational modes is required [7].

The performance of quantum operations with atoms and ions can be improved by ground-state cooling of vibrational degrees of freedom. Thermally induced phase noise and amplitude fluctuations of qubit-qubit interaction can also be suppressed by ground-state cooling, which is essential for realizing high-fidelity quantum gates [13,14] and reliable quantum simulations [15,16]. Moreover, quantum simulations with both vibrational and fermionic degrees of freedom [17,18] naturally demand ground-state cooling of vibrational modes. As the sizes of quantum systems scale up, efficient ground-state cooling for large numbers of modes becomes even more necessary for high-fidelity quantum manipulations.

By removing the entropy from oscillators to photons, laser cooling provides a practical way to prepare the ground state of atomic and even macroscopic oscillators. Laser cooling was first experimentally demonstrated by velocity-dependent radiative force [19,20], which is known as Doppler cooling. The final temperature can be reached with Doppler cooling is limited by the natural linewidth of the cooled atoms. Sisyphus cooling provides a lower temperature than the Doppler limit [21,22], which has been widely used with neutral atoms. Recently, it was found that Sisyphus cooling can also be applied to trapped ions [22]. Although ground-state cooling can be realized by resolved-sideband cooling [23,24], the narrow excitation range of resolved-sideband transitions makes it difficult to perform simultaneous ground-state cooling for multiple motional modes of large crystals. Moreover, some sideband transitions driven by high-power lasers induce a charging problem [25], which is even worse for UV laser beams.

Electromagnetically-induced-transparency (EIT) cooling [26–28] provides an alternative possibility: It can apace cool down a wide range of vibrational modes simultaneously, which has been demonstrated in the linear trap and the Penning trap with tens to hundreds of ions [29,30]. Typical EIT cooling uses quantum interference in a three-level Λ scheme and has been implemented only for ions without clock states. Here, we demonstrate a novel cooling method for $^{171}Yb^{+}$ ions with a clock state, based on double EIT [31–36] in a four-level system. Double-EIT cooling

has been theoretically studied [37–40], and a variant of it has been implemented with $^{40}Ca^{+}$ ion [41]. We experimentally perform double-EIT cooling of $^{171}Yb^{+}$ ions to prepare motional ground states of a two-dimensional (2D) ion crystal. We cool down the transverse modes perpendicular to the crystal plane in which the micromotion oscillates [42]; therefore, the cooling efficiency is negligibly affected by micromotion. The efficiency of double-EIT cooling is systematically studied as a function of various control parameters including the intensity and the detuning of the probe and the driving laser beams to obtain optimal conditions. For multiple motional modes, crystals are cooled down near to their ground states in hundreds of microseconds with cooling rates similar to that of a single ion.

Double-EIT cooling for $^{171}Yb^{+}$ ions involves four energy levels, which is different from EIT cooling in a three-level Λ scheme. As shown in Fig. 1(a), the excited state $|e\rangle \equiv |F=0, m=0\rangle$ in the $P_{1/2}$ manifold is coupled to three states of $|-\rangle \equiv |F=1, m=-1\rangle$, $|0\rangle \equiv |F=1, m=0\rangle$, and $|+\rangle \equiv |F=1, m=+1\rangle$ in the $S_{1/2}$ manifold. The four-level system can be regarded as two Λ schemes, which produce two Fano-like profiles in the absorption spectrum. For instance, one of the Λ schemes consists of the $|-\rangle$, $|0\rangle$ (or $|+\rangle$, $|0\rangle$) states and the excited state $|e\rangle$, which are coupled by the driving beam with σ^{+} (or σ^{-}) polarization and the probe beam with π polarization, respectively. As shown in Fig. 1(b), the absorption spectrum of the probe beam for an ion at rest has two null points corresponding to two dark states when the detuning of the transition $|0\rangle \leftrightarrow |e\rangle$ matches the detuning of the transitions $|\pm\rangle \leftrightarrow |e\rangle$ [43]. And the two narrow peaks correspond to dressed states formed by $|\pm\rangle$ and $|e\rangle$ [43]. We determine the distances between null points and the corresponding narrow peaks by the ac Stark shift of dressed states.

The principle of double-EIT cooling is similar to that of single-EIT cooling, which uses the asymmetric absorption profile to enhance red-sideband transitions and suppress carrier or blue-sideband transitions, as shown in Fig. 1(b). The broad width of the peak enables wide-range cooling. The motional modes of large crystals can be efficiently cooled down to near the ground state based on the unbalanced scattering amplitude between red- and blue-sideband transitions. When the detuning Δ_p of the probe beam is set equal to $\Delta_{\sigma^+} \equiv \Delta_d + \delta_B$, the internal state of the ion is pumped to a dark state, and the ion will not absorb any photon unless the ion motion induces a differential Doppler shift $\vec{v} \cdot (\hat{k}_\pi - \hat{k}_{\sigma^+})/c = \delta_+$ between the π and σ^+ transitions. As stated above, double EIT can cool down only motional modes nonperpendicular to the difference in wave vector $(\hat{k}_\pi - \hat{k}_{\sigma^+})$. Therefore, the net k vector should be aligned to the direction of the motional modes of interest. In our experiment, we choose the right peak for cooling; however, both peaks in the absorption spectrum can be used with similar cooling rates and limits. In principle, it is possible to make only one peak dominant, similar to the simple Λ system, by unbalancing the Rabi

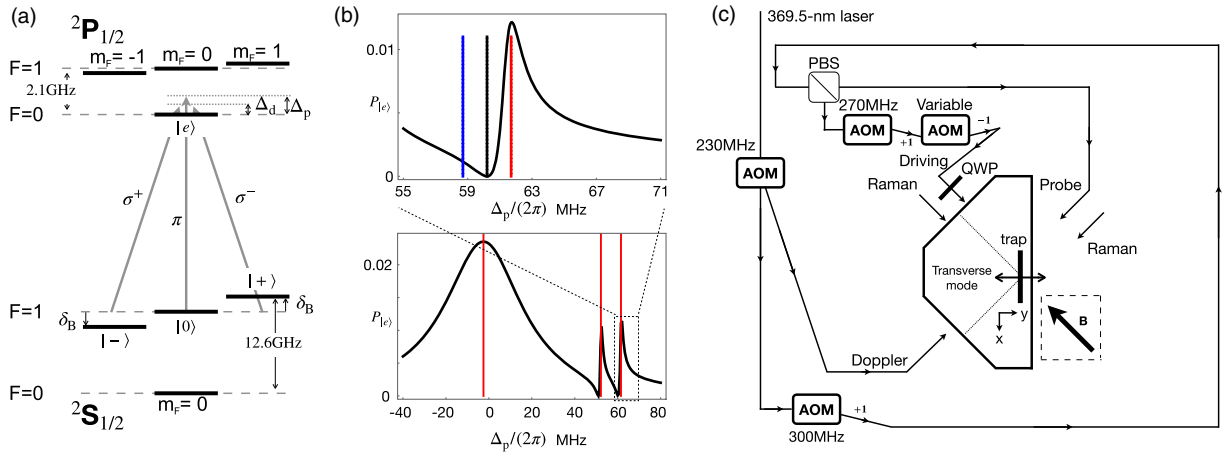

FIG. 1. (a) Relevant energy levels of $^{171}Yb^{+}$ for EIT cooling. (b) Fano-like profile of double EIT. The spectrum is calculated by steady-state solution of the master equation or by scattering amplitude [43]. In the simulation, we set $\Delta_d/(2\pi) = 55.6$ MHz, $\delta_B/(2\pi) = 4.6$ MHz, $\Omega_{\sigma,\pm}/(2\pi) = 17$ MHz, $\Omega_\pi/(2\pi) = 4$ MHz, and $\nu/(2\pi) = 1.5$ MHz, where ν is the frequency of the mode we intend to cool down. The bottom one shows the spectrum in a large range, while the red lines represent theoretical predictions of the positions of dressed states. The top one shows the spectrum around the peak we use for cooling, and the blue (red) line represents the position of the motional sideband, while the dark line represents carrier transition. The red sideband has lower energy, which corresponds to a higher detuning. (c) Optical configuration. The EIT beam is first separated from the Doppler cooling beam with a 14 GHz sideband and then is split into the driving beam and the probe beam by a polarizing beam splitter (PBS). The relative detuning $\Delta_d - \Delta_p$ is controlled by two AOMs acted on the driving beam. The first-order diffraction of the 270 MHz AOM and the negative first order of the variable AOM are used. The net propagating vectors Δk of both the EIT and the Raman beams are along the direction of the transverse mode. A quarter-wave plate (QWP) is used to adjust the polarization of the driving beam.

frequencies of the σ^+ and σ^- components of the driving beam. However, we do not observe an enhancement of cooling efficiency by using an unbalanced driving beam.

We experimentally demonstrate double-EIT cooling with $^{171}Yb^+$ ions, which have a clock-state qubit with a coherence time of over 10 min [50]. The energy splitting ω_0 of the qubit states $|F=1,m=0\rangle$ and $|F=0,m=0\rangle$ in the $S_{1/2}$ manifold is 12.642 812 GHz. The $^{171}Yb^+$ ions are trapped in a pancakelike potential produced by a radio-frequency Paul trap as described in Ref. [42], where trapped ions can form a 2D crystal. A B field of 3.32 G is horizontally applied to break the dark state resonance in Doppler cooling, as shown in Fig. 1(c).

The EIT beams consist of two lasers, which are close to the $S_{1/2}|F=1,m=0\rangle$ to $P_{1/2}|F=0,m=0\rangle$ transition. The EIT beams are aligned to make the difference in wave vectors parallel to the transverse direction of motional modes. One of the beams serves as driving the $\sigma_\pm$ transitions between $|\pm\rangle \leftrightarrow |e\rangle$. The other beam works as a probe beam, which couples the energy levels $|0\rangle \leftrightarrow |e\rangle$. The detuning Δ_p of the probe beam is fixed at $(2\pi)55.6$ MHz, and the detuning Δ_d of the driving beam is adjusted by altering the frequency difference between two acousto-optic modulators (AOMs), as shown in Fig. 1(c). We measure the Rabi frequency and the polarization of the EIT beams by observing the differential ac Stark shift of the clock-state qubit and the Zeeman-state qubits [22,43,44]. The Rabi frequencies $\{\Omega_{\sigma_-},\Omega_\pi,\Omega_{\sigma_+}\}/(2\pi)$ of the driving beam of 24μW and the probe beam of 5.5 μW are {16.74,1.72, 18.03} and {1.49, 6.67, 3.17} MHz, respectively.

Figure 2(a) shows the experimental sequence to study double-EIT cooling with a single ion. For a single $^{171}Yb^+$ ion, secular trap frequencies are $\omega_y/2\pi = 2.38$ MHz in the transverse direction and $\{\omega_x,\omega_z\}/2\pi = \{0.42, 0.47\}$ MHz in the crystal plane. We first apply Doppler cooling, which leads to the Doppler-limit temperatures around phonon number $\bar{n}\approx 7$. After Doppler cooling, 95% population of the internal state of ions falls into the $S_{1/2}|F=1\rangle$ manifold. Afterward, we apply the EIT beams for a duration τ_{EIT}. In order to measure the final phonon number $\bar{n}$, 3 μs optical pumping is carried out to prepare the ground state $S_{1/2}|F=0,m=0\rangle$. By driving blue-sideband transition and fitting time evolution [45], the average phonon number $\bar{n}$ is extracted.

We experimentally study double-EIT cooling dynamics, with relative detuning $\Delta_p - \Delta_d = 4.55$ MHz, by measuring the mean occupation number $\bar{n}$ at various cooling durations τ_{EIT}, as indicated in Fig. 2(b). The mean vibrational number $\bar{n}$ is measured by fitting the blue-sideband transitions, which are shown in Fig. 2(c) before and in Fig. 2(d) after EIT cooling. Without EIT cooling, oscillations on the blue-sideband transition decay fast due to various excitations on different vibrational number states with different Rabi frequencies. As shown in Fig. 2(d), the

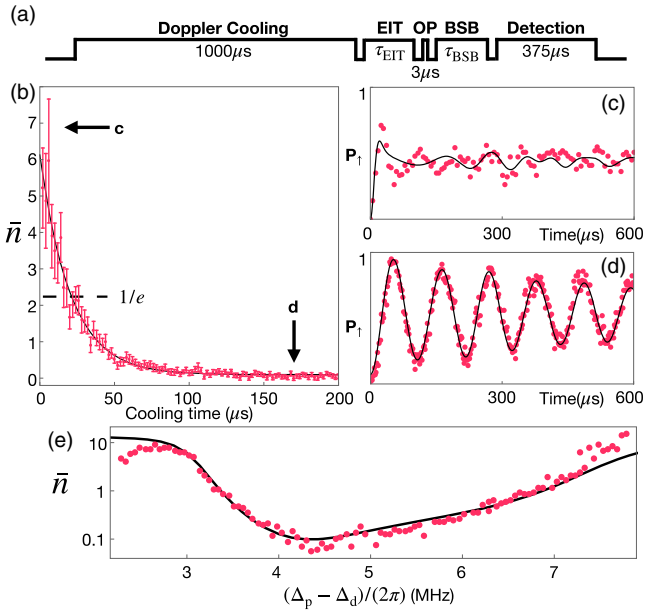

FIG. 2. (a) Experimental sequence for exploring EIT cooling of a single trapped ion. (b) Cooling dynamics for the transverse mode along the y axis. Red points are experimental data obtained by fitting blue-sideband transitions shown in (c) and (d). Error bars denote fitting errors. The black line is an exponential fit. The horizontal dashed line indicates $1/e$ of initial phonon number. (c), (d) The blue-sideband transition after (c) Doppler cooling and (d) EIT cooling of 200 μs. (e) Average phonon number $\bar{n}$ at the end of double-EIT cooling versus the relative detuning between the probe beam and the driving beam. The black line is the numerical simulation result obtained by solving the master equation [43].

minimum value of $\bar{n}_{\mathrm{min}} = 0.06(\pm 0.059)$ of EIT cooling demonstrates a near ground-state cooling similar to sideband cooling. The $1/e$ cooling time $\tau_{\mathrm{cool}} = 1/\gamma_{\mathrm{cool}}$, where γ_{cool} is the cooling rate, is $30(\pm 1.6)$ μs. A duration of 200 μs is sufficient to reach the ground state.

By changing the frequency difference between the EIT beams, we determine the cooling range and the optimal detuning for double-EIT cooling. The efficiency of EIT cooling is determined by the ratio of absorption strengths between red-sideband and blue-sideband transitions, as shown in Fig. 1(b), which is controlled by the detuning of the driving beam Δ_d in our experiment. The optimal detuning $(\Delta_p - \Delta_d)/(2\pi)$ for double-EIT cooling locates at 4.55 MHz. This value is in accordance with the predicted value of 4.57 MHz, which can be calculated by $\delta_B + \delta_{\mathrm{DR}} - \nu$, where $\delta_{\mathrm{DR}} = (2\pi)$ 2.31 MHz is the dressed-state ac Stark shift [43]. Numerical simulations are performed to assess the experimental results, including a heating rate of 0.67 ms^{-1} along the transverse direction. The solid line in Fig. 2(e) indicates the simulated average phonon numbers, which match the experimental results fairly well.

The EIT cooling rate γ_{cool} and the minimum phonon number n_{min} as functions of intensities of the EIT beams are

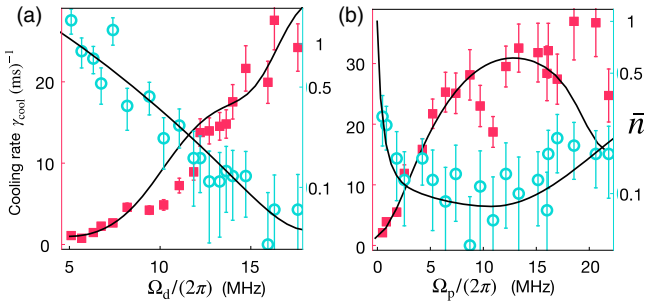

FIG. 3. The final mean phonon numbers (circular points) and the cooling rates (square points) are plotted versus the power of (a) the driving beam and (b) the probe beam. Error bars denote the fitting uncertainties of blue-sideband evolutions, similar to Figs. 2(c) and 2(d). Solid lines are numerical simulation results obtained by solving the master equation [43].

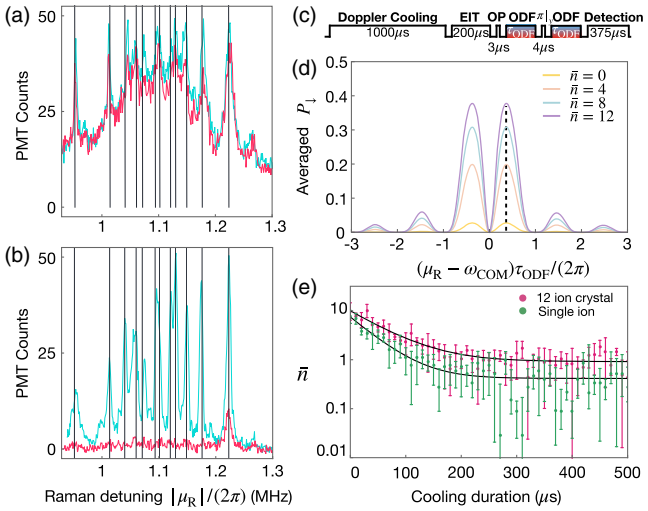

FIG. 4. (a),(b) Blue-sideband (blue curve) and red-sideband (red curve) spectrum after (a) Doppler cooling and (b) EIT cooling. The vertical axis represents the count globally collected by the photomultiplier tube (PMT). The horizontal axis $\mu_R = \omega_R - \omega_0$ is the detuning of the Raman transition from the qubit transition. Vertical lines indicate the locations of 12 motional modes perpendicular to the 2D-crystal plane. (c) Pulse sequence for the ODF thermometry. (d) ODF spectrum with different average phonon numbers. The dashed black line indicates the position we choose for the cooling rate measurement. (e) Cooling dynamics for a single ion (green) and a 2D crystal with 12 ions (red). The dots are experimental data. The error bars represent the standard deviation induced by the quantum projection noise. Solid lines are fitting curves by exponential decay functions.

shown in Fig. 3. We characterize the cooling efficiency as the power of the driving (probe) beam varies, while the power of the probe (driving) beam is fixed at 5.5 μW, $\Omega_p/2\pi = 6.67$ MHz (24 μW, $\Omega_d/2\pi = 17.39$ MHz). At each point of laser powers, we search the optimal EIT detuning $(\Delta_p - \Delta_d)$. As shown in Fig. 3, numerical simulations match the experimental results fairly well, while the discrepancies of cooling rates could originate from the overall power fluctuations. As the power of the driving beam increases to the maximal possible value in our experiment, the cooling efficiency is also enhanced, as shown in Fig. 3(a). On the other hand, Fig. 3(b) shows that both the cooling rate and limit have a local optimum. To balance the cooling rate and limit, we determine the optimal power of the probe beam by minimizing the ratio between the final phonon number and cooling rate of the numerical curve in Fig. 3(b). Finally, we found $\Omega_p/(2\pi) = 11$ MHz is optimal for cooling.

To assess double-EIT cooling on a large ion crystal, we store a 2D crystal of 12 ions in a pancake harmonic potential with secular trap frequencies $\omega_y/(2\pi) = 1.22$ MHz in the transverse direction and $\{\omega_x, \omega_z\}/(2\pi) = \{0.34, 0.42\}$ MHz in the crystal plane. With this smaller ω_y, the heating rate is increased to 0.77 ms^{-1}. We suppress the micromotion of the 2D crystal in the transverse modes by adjusting the plane of the crystal to be in line with the micromotion direction, which is the z axis shown in Fig. 1(c). Then, the direction of dominant micromotion is perpendicular to directions of the transverse modes and the net-propagation direction of the EIT beams. In such a situation, the effect of micromotion is eliminated in double-EIT cooling; therefore, we can perform efficient cooling. Indeed, we measure the strength of the micromotion sideband in the Raman spectroscopy and observe it is at a similar level to a single ion [42]. Double-EIT cooling of a 12-ion crystal is observed from the Raman absorption spectrum. Figure 4(a) depicts the spectrum with only Doppler cooling, where the peaks of blue-sideband (blue curve) and red-sideband (red curve) transitions possess similar heights across all motional modes, which indicates the phonon numbers are much larger than 1. Figure 4(b) shows the spectrum after both Doppler and EIT cooling, where the reduction of red-sideband transitions indicates simultaneous ground-state cooling of all transverse modes. The small peak in the spectrum of red-sideband transitions originates from imperfect ground-state cooling of the center of mass (COM) mode with linearly scaled heating rate. We numerically simulate the red-sideband absorption spectrum of the crystal in the vicinity of each mode for the parameters of our experiment [29]. The estimated phonon number of the COM mode is 1.04 ($\pm$0.26) [43].

We also use the optical-dipole-force (ODF) thermometry [46] to measure the final phonon number of the COM mode. The ODF is generated by simultaneously driving red-sideband and blue-sideband transitions, where the $\sigma_x\sigma_x$ interaction emerges. With ion-phonon coupling, this $\sigma_x\sigma_x$ interaction could induce decoherence in the x basis. The Ramsey measurement is adopted to probe this decoherence, as shown in Fig. 4(c). We first prepare all qubits to their ground state in the σ_z basis $|\downarrow\rangle_z$ and then apply the ODF for two fixed durations τ_{ODF} with a spin-echo pulse sandwiched in between. Figure 4(d) shows the spectrum near the COM mode of the crystal with different phonon

numbers. The temperature of the crystal is measured by fitting the spectrum to the formula [Eq. (35)] in Ref. [43], where the $\bar{n}$ of Doppler cooling and EIT cooling are $10.72(\pm 4.23)$ and $1.04(\pm 0.61)$, respectively. Here, we calibrate the strength of the ODF beams by measuring the Lamb-Dicke parameter and the Rabi frequency of carrier transition [43].

To explore the cooling dynamics for the COM mode of a crystal with 12 ions, we develop a simple method to estimate $\bar{n}$ instead of using the whole ODF spectrum in Fig. 4(d). By fixing the detuning at the position with the largest decoherence, the height of the ODF signal is converted to the mean phonon number $\bar{n}$ [43]. We observe a cooling rate and a cooling limit consistent with the rate and the limit of a single ion. In the setting of 12 ions, the cooling rate and the limit of a single ion are measured as $22.1(\pm 0.1)$ ms^{-1} and $0.34(\pm 0.25)$, respectively, as shown in Fig. 4(e). With 12 ions, the rate and the limit are $15.9(\pm 0.1)$ ms^{-1} and $1.04(\pm 0.61)$, respectively. The cooling rate is reduced, and the cooling limit is increased for 12 ions due to the heating rates proportional to the number of ions, which is $0.61(\pm 0.08)$ ms^{-1} per ion [43]. In our experiment, we do not observe the more efficient EIT cooling due to the many-body effect reported in Refs. [30,51] within our error bars, which may need further experimental or theoretical study.

In summary, we have experimentally shown that double-EIT cooling can be performed with $^{171}\mathrm{Yb}^{+}$ ions and used to efficiently cool down the transverse motional modes of a 2D crystal. We demonstrate that EIT cooling can be realized for atoms and ions with more complicated level structures than a Λ scheme. Our experimental approach is suitable for other hyperfine ions with a clock state, offering a fast ground-state cooling technology for atoms with a long coherence time. This method may be useful for a large-scale trapped ion quantum processor, for use in quantum computation, quantum magnetism, quantum chemistry, and quantum machine learning. In future work, it would be interesting to engineer the absorption spectrum for more efficient cooling [41] and to study whether the in-plane modes of 2D crystals can be efficiently cooled down to near the ground state.

We thank Paul Haljan, Dzmitry Matsukevich, Yiheng Lin, John Bollinger, Athreya Shankar, and Christian Roos for their helpful discussion. We acknowledge the use of the Quantum Toolbox in PYTHON (QuTiP) [52]. This work was supported by the National Key Research and Development Program of China under Grants No. 2016YFA0301900 and No. 2016YFA0301901 and the National Natural Science Foundation of China Grants No. 11374178, No. 11574002, and No. 11974200.

*mu.q.phys@gmail.com
†kimkihwan@mail.tsinghua.edu.cn

[1] D. J. Wineland, Rev. Mod. Phys. **85**, 1103 (2013).
[2] S. Lloyd and S. L. Braunstein, Phys. Rev. Lett. **82**, 1784 (1999).
[3] H.-K. Lau and M. B. Plenio, Phys. Rev. Lett. **117**, 100501 (2016).
[4] S. Ding, G. Maslennikov, R. Hablützel, H. Loh, and D. Matsukevich, Phys. Rev. Lett. **119**, 150404 (2017).
[5] S. Ding, G. Maslennikov, R. Hablützel, and D. Matsukevich, Phys. Rev. Lett. **119**, 193602 (2017).
[6] C. Flühmann, T. L. Nguyen, M. Marinelli, V. Negnevitsky, K. Mehta, and J. Home, Nature (London) **566**, 513 (2019).
[7] S. Aaronson and A. Arkhipov, in *Proceedings of the 43rd Annual ACM Symposium on Theory of Computing, STOC '11* (ACM, New York, 2011), p. 333.
[8] H.-K. Lau and D. F. V. James, Phys. Rev. A **85**, 062329 (2012).
[9] C. Shen, Z. Zhang, and L.-M. Duan, Phys. Rev. Lett. **112**, 050504 (2014).
[10] K. Toyoda, R. Hiji, A. Noguchi, and S. Urabe, Nature (London) **527**, 74 (2015).
[11] M. Um, J. Zhang, D. Lv, Y. Lu, S. An, J.-N. Zhang, H. Nha, M. Kim, and K. Kim, Nat. Commun. **7**, 11410 (2016).
[12] Y. Shen, Y. Lu, K. Zhang, J. Zhang, S. Zhang, J. Huh, and K. Kim, Chem. Sci. **9**, 836 (2018).
[13] C. J. Ballance, T. P. Harty, N. M. Linke, M. A. Sepiol, and D. M. Lucas, Phys. Rev. Lett. **117**, 060504 (2016).
[14] T. P. Harty, M. A. Sepiol, D. T. C. Allcock, C. J. Ballance, J. E. Tarlton, and D. M. Lucas, Phys. Rev. Lett. **117**, 140501 (2016).
[15] R. Blatt and C. F. Roos, Nat. Phys. **8**, 277 (2012).
[16] C. Monroe, W. Campbell, L.-M. Duan, Z.-X. Gong, A. Gorshkov, P. Hess, R. Islam, K. Kim, G. Pagano, P. Richerme *et al.*, arXiv:1912.07845.
[17] A. Mezzacapo, J. Casanova, L. Lamata, and E. Solano, Phys. Rev. Lett. **109**, 200501 (2012).
[18] D. Lv, S. An, Z. Liu, J.-N. Zhang, J. S. Pedernales, L. Lamata, E. Solano, and K. Kim, Phys. Rev. X **8**, 021027 (2018).
[19] D. J. Wineland, R. E. Drullinger, and F. L. Walls, Phys. Rev. Lett. **40**, 1639 (1978).
[20] W. Neuhauser, M. Hohenstatt, P. Toschek, and H. Dehmelt, Phys. Rev. Lett. **41**, 233 (1978).
[21] J. Dalibard and C. Cohen-Tannoudji, J. Opt. Soc. Am. B **6**, 2023 (1989).
[22] S. Ejtemaee and P. C. Haljan, Phys. Rev. Lett. **119**, 043001 (2017).
[23] C. Monroe, D. M. Meekhof, B. E. King, S. R. Jefferts, W. M. Itano, D. J. Wineland, and P. Gould, Phys. Rev. Lett. **75**, 4011 (1995).
[24] C. Roos, T. Zeiger, H. Rohde, H. C. Nägerl, J. Eschner, D. Leibfried, F. Schmidt-Kaler, and R. Blatt, Phys. Rev. Lett. **83**, 4713 (1999).
[25] M. Harlander, M. Brownnutt, W. Hänsel, and R. Blatt, New J. Phys. **12**, 093035 (2010).
[26] G. Morigi, J. Eschner, and C. H. Keitel, Phys. Rev. Lett. **85**, 4458 (2000).
[27] C. F. Roos, D. Leibfried, A. Mundt, F. Schmidt-Kaler, J. Eschner, and R. Blatt, Phys. Rev. Lett. **85**, 5547 (2000).
[28] Y. Lin, J. P. Gaebler, T. R. Tan, R. Bowler, J. D. Jost, D. Leibfried, and D. J. Wineland, Phys. Rev. Lett. **110**, 153002 (2013).

[29] R. Lechner, C. Maier, C. Hempel, P. Jurcevic, B. P. Lanyon, T. Monz, M. Brownnutt, R. Blatt, and C. F. Roos, Phys. Rev. A **93**, 053401 (2016).
[30] E. Jordan, K. A. Gilmore, A. Shankar, A. Safavi-Naini, J. G. Bohnet, M. J. Holland, and J. J. Bollinger, Phys. Rev. Lett. **122**, 053603 (2019).
[31] E. Paspalakis and P. Knight, J. Opt. B **4**, S372 (2002).
[32] S. Beck and I. E. Mazets, Phys. Rev. A **95**, 013818 (2017).
[33] H. M. M. Alotaibi and B. C. Sanders, Phys. Rev. A **89**, 021802(R) (2014).
[34] B. S. Ham and P. R. Hemmer, Phys. Rev. Lett. **84**, 4080 (2000).
[35] M.-J. Lee, J. Ruseckas, C.-Y. Lee, V. Kudriašov, K.-F. Chang, H.-W. Cho, G. Juzeliānas, and A. Y. Ite, Nat. Commun. **5**, 5542 (2014).
[36] D. Wang, C. Liu, C. Xiao, J. Zhang, H. M. M. Alotaibi, B. C. Sanders, L.-G. Wang, and S. Zhu, Sci. Rep. **7**, 5796 (2017).
[37] J. Evers and C. H. Keitel, Europhys. Lett. **68**, 370 (2004).
[38] Z. Yi, W.-J. Gu, and G.-X. Li, Opt. Express **21**, 3445 (2013).
[39] T. Huang, Y. Qi, F. Zhou, Y. Niu, and S. Gong, Opt. Int. J. Light Electron Opt. **127**, 2978 (2016).
[40] I. Semerikov, I. Zalivako, A. Borisenko, K. Khabarova, and N. Kolachevsky, J. Russ. Laser Res. **39**, 568 (2018).
[41] N. Scharnhorst, J. Cerrillo, J. Kramer, I. D. Leroux, J. B. Wübbena, A. Retzker, and P. O. Schmidt, Phys. Rev. A **98**, 023424 (2018).
[42] Y. Wang, M. Qiao, Z. Cai, K. Zhang, N. Jin, P. Wang, W. Chen, C. Luan, H. Wang, Y. Song *et al.*, arXiv:1912.04262.
[43] See Supplemental Material at http://link.aps.org/supplemental/10.1103/PhysRevLett.126.023604 for more details on the theory of double-EIT cooling, the calibration of the ac Stark shift, and the measurement of the phonon number, which includes Refs. [44–49].
[44] H. Häffner, S. Gulde, M. Riebe, G. Lancaster, C. Becher, J. Eschner, F. Schmidt-Kaler, and R. Blatt, Phys. Rev. Lett. **90**, 143602 (2003).
[45] D. Leibfried, R. Blatt, C. Monroe, and D. Wineland, Rev. Mod. Phys. **75**, 281 (2003).
[46] B. C. Sawyer, J. W. Britton, A. C. Keith, C. C. Joseph Wang, J. K. Freericks, H. Uys, M. J. Biercuk, and J. J. Bollinger, Phys. Rev. Lett. **108**, 213003 (2012).
[47] B. Lounis and C. Cohen-Tannoudji, J. Phys. II **2**, 579 (1992).
[48] D. Hayes, D. N. Matsukevich, P. Maunz, D. Hucul, Q. Quraishi, S. Olmschenk, W. Campbell, J. Mizrahi, C. Senko, and C. Monroe, Phys. Rev. Lett. **104**, 140501 (2010).
[49] Q. A. Turchette, D. Kielpinski, B. E. King, D. Leibfried, D. M. Meekhof, C. J. Myatt, M. A. Rowe, C. A. Sackett, C. S. Wood, W. M. Itano, C. Monroe, and D. J. Wineland, Phys. Rev. A **61**, 063418 (2000).
[50] Y. Wang, M. Um, J. Zhang, S. An, M. Lyu, J.-N. Zhang, L.-M. Duan, D. Yum, and K. Kim, Nat. Photonics **11**, 646 (2017).
[51] A. Shankar, E. Jordan, K. A. Gilmore, A. Safavi-Naini, J. J. Bollinger, and M. J. Holland, Phys. Rev. A **99**, 023409 (2019).
[52] J. R. Johansson, P. D. Nation, and F. Nori, Comput. Phys. Commun. **184**, 1234 (2013).